

Clustering of SNPs along a chromosome: can the neutral model be rejected?

Anders Eriksson¹, Bernhard Haubold², and Bernhard Mehlig¹

November 13, 2018

¹Physics & Engineering Physics, Chalmers/GU, Gothenburg, Sweden

²LION Bioscience AG, Waldhofer Str. 98, 69123 Heidelberg, Germany

Running Title: SNP Clustering

Key Words: neutrality, reciprocal recombination, single nucleotide polymorphism, infinite sites model, clustering

Abstract

Single nucleotide polymorphisms (SNPs) often appear in clusters along the length of a chromosome. This is due to variation in local coalescent times caused by, for example, selection or recombination. Here we investigate whether recombination alone (within a neutral model) can cause statistically significant SNP clustering. We measure the extent of SNP clustering as the ratio between the variance of SNPs found in bins of length l , and the mean number of SNPs in such bins, σ_l^2/μ_l . For a uniform SNP distribution $\sigma_l^2/\mu_l = 1$, for clustered SNPs $\sigma_l^2/\mu_l > 1$. Apart from the bin length, three length scales are important when accounting for SNP clustering: The mean distance between neighboring SNPs, Δ , the mean length of chromosome segments with constant time to the most recent common ancestor, ℓ_{seg} , and the total length of the chromosome, L . We show that SNP clustering is observed if $\Delta < \ell_{\text{seg}} \ll L$. Moreover, if $l \ll \ell_{\text{seg}} \ll L$, clustering becomes independent of the rate of recombination. We apply our results to the analysis of SNP data sets from mice, and human chromosomes 6 and X. Of the three data sets investigated, the human X chromosome displays the most significant deviation from neutrality.

INTRODUCTION

Single nucleotide polymorphisms (SNPs) are the most abundant polymorphisms in most populations. Due to their ubiquity and stability they are useful in the diagnosis of human diseases (ZHOU *et al.*, 2002), detection of human disease genes (WILLEY *et al.*, 2002), and gene mapping in organisms as diverse as humans (MCINNES *et al.*, 2001), *Arabidopsis thaliana* (CHO *et al.*, 1999), and *Drosophila* (BERGER *et al.*, 2001). For this reason, several large-scale SNP-mapping projects are currently under way in eukaryotic model organisms including *A. thaliana* (<http://arabidopsis.org/Cereon>), *Drosophila* (HOSKINS *et al.*, 2001), mouse (LINDBLAD-TOH *et al.*, 2000), and human (INTERNATIONAL HUMAN GENOME SEQUENCING CONSORTIUM, 2001; THE INTERNATIONAL SNP MAP WORKING GROUP, 2001).

A central question in the analysis of data collected in the context of these projects is how SNPs

are distributed along a chromosome and what inferences about selection might be drawn from this distribution. This question can be addressed at the level of individual polymorphisms (FAY *et al.*, 2001) or at the level of the whole genome (LINDBLAD-TOH *et al.*, 2000).

LINDBLAD-TOH *et al.* (2000) have observed that SNPs cluster along chromosomes in mice. This clustering may either be due to variation in local mutation rates, or variation in local coalescent times. The hypothesis of local differences in mutation rates in mice was rejected, leaving differences in local coalescent times as the most likely explanation of SNP clustering. In the case of the mouse genome such variation in coalescent times may be due to selection in the wild or selection for unusual coat colors (c.f. breeding of ‘fancy’ mice in the eighteenth and nineteenth centuries). Another possibility mentioned is the effect of inbreeding (LINDBLAD-TOH *et al.*, 2000).

On the other hand, recombination alone leads to fluctuations in the time to the most recent common ancestor along a chromosome (HUDSON, 1990). Since time to the most recent common ancestor is proportional to the number of SNPs found in the respective chromosome segment, recombination in a neutral model might be sufficient to account for genome-wide SNP clustering.

A well established stochastic model for neutral genetic variation is the constant-rate mutation coalescent process under the infinite-sites model. According to this model, the total number of SNPs found in a sample is expected to be Poisson distributed with parameter $\lambda = \theta T_{\text{tot}}/2$, where T_{tot} is the total time to the most recent common ancestor, $\theta = 4N_e u$, u is the probability of mutation per site per generation, and N_e is the effective population size (see HUDSON (1990) for a review). This is a *global* property of any contiguous stretch of DNA, and holds in the absence of recombination, where all sites have the same genealogy (and thus the total time T_{tot} to the most recent common ancestor is constant along the chromosome). In the presence of recombination, the number of polymorphisms conditional on the genealogies of all sites is still Poisson distributed with parameter

$$\frac{\theta}{2} \int_0^L dx T_{\text{tot}}(x). \quad (1)$$

Here x denotes the position on, and L the length of the chromosome. Since the value of parameter (1) fluctuates between samples, the total number of SNPs is no longer Poisson distributed, except in the case of very frequent recombination where the variance of this parameter tends to zero. These properties of the coalescent are reviewed in HUDSON (1990). For more recent reviews see NORDBORG (2001) and NORDBORG and TAVARÉ (2002).

In this paper we investigate *local* SNP statistics: local spatial fluctuations in $T_{\text{tot}}(x)$ due to recombination (HUDSON, 1990) may give rise to *local* variations in the SNP density. Here we study the implications of this idea for the analysis of experimental SNP data.

Specifically, we address the following five questions. How significant is SNP clustering caused by recombination? How does the clustering depend on the parameters of the model (the sample size, the mutation rate, and the recombination rate)? On which length scales are such clusters expected? How does the clustering depend on the length scale on which it is observed? Finally, can recombination alone account for the clustering of SNPs observed in mice (LINDBLAD-TOH *et al.*, 2000), or in the human genome (THE INTERNATIONAL SNP MAP WORKING GROUP, 2001)? In the following these questions are answered by analyzing coalescent simulations.

MODEL AND METHODS

We use coalescent simulations under the neutral infinite-sites model to generate allele samples (HUDSON, 1990; NORDBORG, 2001). As usual, this model incorporates mutation (with rate $\theta = 4N_e u$) and reciprocal recombination (with rate $R = 4N_e r$, where r is the probability of a recombination event per generation per sequence).

The coalescent process generates genealogies for all sites of the n sequences in a given sample. In the absence of recombination, these genealogies are identical for all sites x . In particular, the total time to the most recent common ancestor T_{tot} is the same for all sites. For a given genealogy, mutations are generated as a Poisson process with rate $\lambda = \theta T_{\text{tot}}/2$. This implies that the density of SNPs along the genome is uniform: in this case SNPs do not cluster.

If the recombination rate is non-zero, the total time to the most recent common ancestor, $T_{\text{tot}}(x)$, varies as a function of the position x (HUDSON, 1990). This corresponds to fluctuating local mutation rates $\lambda(x) = \theta T_{\text{tot}}(x)/2$. In the presence of recombination, the distribution of SNPs is thus determined by a Poisson process in x with fluctuating rates $\lambda(x)$. Figure 1 shows such a process for realizations of $\lambda(x)$ corresponding to three different sets of parameter values. The fluctuating rates $\lambda(x)$ are shown as solid lines. Note that $\lambda(x)$ is constant over segments of the chromosome which are identical by descent (called MRCA segments in the following). The figure illustrates possible local clustering of SNPs as a consequence of local variation in $\lambda(x)$ due to recombination. While the density of SNPs in the top and bottom panels is uniform, the middle panel exhibits clustering in regions of high $\lambda(x)$.

In the remainder of this paper, the local clustering such as that exhibited in the middle panel of Figure 1 is described quantitatively. It is customary in experimental SNP surveys to count SNPs in bins of length l . Such a bin might, for example, correspond to a sequence tagged site (STS), or some arbitrarily chosen stretch of sequence. The mean number of SNPs per bin is then

$$\mu_l = \frac{1}{N_{\text{bins}}} \sum_{j=1}^{N_{\text{bins}}} n_j(l) \quad (2)$$

and its variance

$$\sigma_l^2 = \frac{1}{N_{\text{bins}} - 1} \sum_{j=1}^{N_{\text{bins}}} (n_j(l) - \mu_l)^2, \quad (3)$$

where $n_j(l)$ is the number of SNPs in bin j and N_{bins} is the total number of bins surveyed (c.f. Figure 2). In some SNP studies, the bins are arranged contiguously along the chromosome (as depicted in Figure 2), in some cases the bins are randomly distributed, or equidistributed but non-contiguous.

We compare empirical values for σ_l^2/μ_l with results of coalescent simulations. In these simulations we determine the ensemble average (denoted by $\langle \sigma_l^2 \rangle$ in the following) and the distribution of σ_l^2 over random genealogies with mutations. We keep the total number of mutations, S , fixed to the empirical value. The local rates $\lambda(x)$ are then given by

$$\lambda(x) = (S/L) T_{\text{tot}}(x)/2, \quad (4)$$

and the value of μ_l is constant between different realizations of the ensemble. One has $\mu_l = l/\Delta$ where $\Delta \equiv L/S$ is the mean distance between neighboring SNPs¹. For uniformly distributed

¹If S fluctuates from sample to sample, $\Delta = L/\langle S \rangle = \left[\theta \sum_{k=1}^{n-1} k^{-1} \right]^{-1}$. Here n is the sample size.

SNPs generated with an x -independent rate, $\sigma_l^2/\mu_l = 1$. In the case of fluctuating rates

$$\sigma_l^2/\mu_l > 1 \quad (5)$$

is expected, since spatial fluctuations of $\lambda(x)$ give rise to an increased ‘‘compressibility’’ of the sequence of SNPs. In other words, σ_l^2/μ_l measures the ‘‘compressibility’’ of the sequence of SNPs: the larger σ_l^2/μ_l , the more significant SNP clustering is on scales l and larger.

To meaningfully speak about SNP clustering, it is necessary that Δ is much smaller than L . This is the case considered in the following. In addition, we assume that bins are much shorter than the chromosome on which they are placed, i.e., we make the following assumptions

$$l \ll L \quad \text{and} \quad \Delta \ll L. \quad (6)$$

It is clear (Figure 1) that the statistical properties of σ_l^2/μ_l crucially depend on how rapidly the rate $\lambda(x)$ fluctuates as a function of x . It is convenient to define a length scale ℓ_{seg} as the ratio of L and the (average) number of jumps of $\lambda(x)$ along the total length of the chromosome. This length scale corresponds to the average MRCA segment length in Figure 1. Here the average is over the chromosome for a given realization of $\lambda(x)$ as well as over an ensemble of such realizations; ℓ_{seg} depends on the recombination rate R , the sample size n , and L (GRIFFITHS and MARJORAM, 1997). The relative sizes of the mean spacing Δ between neighboring SNPs, of the bin size l , the chromosome length L , and of the average MRCA segment length ℓ_{seg} will play a crucial role in determining SNP clustering.

In the following section, we analyze local SNP clustering in the model described above. We determine the significance of the four length scales Δ , l , ℓ_{seg} , and L for the statistics of the observable σ_l^2/μ_l and analyze for which parameter values θ , R , and on which length scales SNP clustering due to recombination is expected to be most significant. In the final section, we discuss the implications of our results in relation to genome-wide surveys of SNPs in mice and humans.

ANALYSIS OF SNP CLUSTERING

Characterization of the spatial fluctuations of $\lambda(x)$: For a given genealogy under the neutral infinite-sites model with recombination SNPs are distributed according to an inhomogeneous Poisson process, that is, according to a Poisson process with a rate $\lambda(x)$ varying along the chromosome (see Figures 1b and c). Given the function $\lambda(x)$, the probability of observing $n(l) = k$ SNPs in bin $[0, l]$ is

$$P(n(l) = k | \lambda(x)) = \frac{1}{k!} \left(\int_0^l dx \lambda(x) \right)^k \exp \left(- \int_0^l dx \lambda(x) \right). \quad (7)$$

Moreover, given the function $\lambda(x)$, counts of SNPs in non-overlapping bins are statistically independent.

Theoretical predictions are computed as ensemble averages over random genealogies, corresponding to averages over random functions $\lambda(x)$. These ensemble averages introduce correlations in the combined process. Such correlations may be weak, but they can be long-ranged. Their range is determined by the length scale on which the random rate $\lambda(x)$ varies. As Figure 1 shows, $\lambda(x)$ is a piecewise constant function: along an MRCA segment the rate is constant, and varies between MRCA segments. The three panels in Figure 1 correspond to the three cases

$\ell_{\text{seg}} = L$ (a), $\Delta \ll \ell_{\text{seg}} \ll L$ (b), and $\ell_{\text{seg}} \ll \Delta$ (c). The average MRCA segment length depends on the sample size n as well as on the recombination rate R . According to GRIFFITHS and MARJORAM (1997)

$$\ell_{\text{seg}} = L \{1 + [1 - 2R/n/(n + 1)]\}^{-1}, \quad (8)$$

where the denominator denotes the expected number of changes of ancestor along the chromosome [notice that eq. (8) does not describe the expected number of sites with the same MRCA as pointed out by WIUF and HEIN (1999)]. The length ℓ_{seg} describes the scale on which the correlations between local mutation rates $\lambda(x)$ decay. For $x < \ell_{\text{seg}}$ these correlations are strong. For $x \gg \ell_{\text{seg}}$, on the other hand, the correlation function

$$C(x) = \frac{\langle \lambda(y)\lambda(y+x) \rangle - \langle \lambda(y) \rangle^2}{\langle \lambda^2(y) \rangle - \langle \lambda(y) \rangle^2} \quad (9)$$

decays to zero. KAPLAN and HUDSON (1985) have shown that correlations between the times T_{tot} pertaining to two loci in an m -locus model decay according to C^{-1} for large values of C (here C is the recombination rate between those loci). Identifying C with an effective recombination rate $R_{\text{eff}} = xR/L$ (where R is the recombination rate between the ends of the chromosome) one concludes that $C(x)$ decays as x^{-1} for large x . In summary, for any finite value of R , correlations between local mutation rates are large on scales up to ℓ_{seg} , and decay for larger distances. These correlations may affect the fluctuations of σ_l^2 .

Fluctuations of σ_l^2 : The empirical observable σ_l^2/μ_l is expected to fluctuate from sample to sample². Since correlations between $\lambda(y)$ and $\lambda(y+x)$ decay as $|x|$ grows, the fluctuations of σ_l^2/μ_l tend to zero in the limit of infinite L (with ℓ_{seg} and l constant):

$$\lim_{\substack{L \rightarrow \infty \\ \ell_{\text{seg}}, l \text{ finite}}} \sigma_l^2/\mu_l = \langle \sigma_l^2 \rangle / \mu_l. \quad (10)$$

In this limit the process is thus self-averaging (ergodic): eq. (10) implies that the averages of $n(l)$ and of its moments along the chromosome equal the ensemble averages $\langle n(l) \rangle$ of $n(l)$ (and of its moments), see also (PLUZHNIKOV and DONNELLY, 1996). Here $n(l)$ is the SNP count in one bin of a given sample, and the ensemble average is taken over random genealogies with mutations. For the case where $n = 2$, $\langle n^2(l) \rangle$ can be derived from eq. (15) in (HUDSON, 1990) by replacing the recombination rate in this equation with lR/L . One obtains

$$\begin{aligned} \sigma_l^2/\mu_l \simeq & 1 + \frac{l}{\Delta} \frac{2}{C^2} \left[-C + \frac{23C + 101}{2\sqrt{97}} \log \left(\frac{2C + 13 - \sqrt{97} \sqrt{13 + \sqrt{97}}}{2C + 13 + \sqrt{97} \sqrt{13 - \sqrt{97}}} \right) \right. \\ & \left. + \frac{C - 5}{2} \log \left(\frac{C^2 + 13C + 18}{18} \right) \right] \end{aligned} \quad (11)$$

with $C = lR/L$. Eq. (11) is approximate (it was derived for an m -site model in which each site obeys the infinite-sites assumption, in the limit of $m \rightarrow \infty$).

When L is large (much larger than l and ℓ_{seg}) but finite, the distribution of σ_l^2/μ_l is expected to be narrow, since σ_l^2/μ_l itself is an average over a large number of (approximately) independent bins. When the sample-to-sample variations of σ_l^2/μ_l are small, theoretical models for SNP

²In our simulations σ_l^2 does, but μ_l does not, since S and L are constant.

clustering are easily tested (and possibly rejected). Empirically determined observables [such as, for example, the variance in the number of loci that differ between pairs of haplotypes in (HAUBOLD *et al.*, 2002)] often have broad distributions; it is thus significant that in recent years longer and longer contiguous chromosome segments have been sequenced and locally averaged observables such as σ_l^2/μ_l are now available. In empirical studies usually $l \ll L$. Consequently, it is the ratio ℓ_{seg}/L which determines the statistics of σ_l^2/μ_l .

As pointed out above, recent empirical data for σ_l^2 were obtained for contiguous non-overlapping bins [as depicted in Figure 2 (THE INTERNATIONAL SNP MAP WORKING GROUP, 2001)]. In other cases, however, the bins were randomly distributed over the chromosome (LINDBLAD-TOH *et al.*, 2000), or equally spaced but far apart from each other (THE INTERNATIONAL SNP MAP WORKING GROUP, 2001). How does the statistics of σ_l^2 depend on the number and the distribution of bins over the chromosome? The expected value of σ_l^2 is independent of the distribution of bins [if $l, \ell_{\text{seg}} \ll L$ it is approximately given by eq. (11)]. The fluctuations of σ_l^2 , however, critically depend on the number and distributions of bins. The following analysis is performed assuming contiguous bins. When comparing with empirical data, however, confidence intervals for σ_l^2/μ_l were obtained using the empirical number and distribution of bins.

Finally, as ℓ_{seg} approaches L , the fluctuations of σ_l^2/μ_l are expected to increase. In the absence of recombination ($\ell_{\text{seg}} = L$), SNPs are distributed according to a Poisson process and the fluctuations tend to zero (if $l \ll L$).

SNP clustering: We have determined the fluctuations of σ_l^2/μ_l using coalescent simulations for sample size $n = 2$, proceeding in five steps: (1) generate a large number of samples of sequence pairs of length L [the results discussed below correspond to values of L ranging between 10^6 and $1.6 \cdot 10^8$ bp]; (2) determine the SNPs within each sample (each pair of sequences); (3) assign the SNPs to contiguous bins as illustrated in Figure 2; (4) calculate σ_l^2/μ_l for each sample; (5) finally, average over samples.

In these coalescent simulations, the bin size l was taken to be much smaller than L , corresponding to, say the length of an STS compared to that of a mouse chromosome. Figure 3a shows the results of coalescent simulations in comparison with eqs. (11) and (14). In keeping with the above discussion, eq. (11) is adequate when ℓ_{seg} is much smaller than L . In this regime, the fluctuations of σ_l^2/μ_l are small (but finite since $N_{\text{bins}} = L/l$ is finite). As ℓ_{seg} approaches L , eqs. (11) and (14) are inappropriate, and the fluctuations increase significantly, as expected.

Three qualitative observations emerge from our simulations:

1. in the region $\Delta < \ell_{\text{seg}} \ll L$, the observed values of σ_l^2/μ_l are larger than unity. If ℓ_{seg} is much smaller than Δ , or if ℓ_{seg} approaches L , $\sigma_l^2/\mu_l \rightarrow 1$;
2. for small values of l , σ_l^2/μ_l exhibits a plateau for intermediate values of ℓ_{seg} (indicated by a dashed line in Figure 3a);
3. for larger values of l , the plateau disappears.

These qualitative observations can be understood as follows.

1. In the absence of recombination, where $\ell_{\text{seg}} = L$, a uniform SNP distribution is expected. In this case

$$\sigma_l^2/\mu_l = 1 \quad (12)$$

[contradicted by equation (12)? and if not, why not?] as pointed out above. Conversely, if ℓ_{seg} is much smaller than l and Δ , the Poisson process averages over the fluctuating local rates $\lambda(x)$. One thus expects [see eq. (7)] local uniformity of SNPs with rate

$$\frac{1}{l} \int_x^{x+l} dx' \lambda(x'). \quad (13)$$

Again, $\sigma_l^2/\mu_l = 1$. In contrast, in the regime $\Delta < \ell_{\text{seg}} \ll L$ significant SNP clustering is observed.

2. Consider the situation $l \ll \ell_{\text{seg}} \ll L$. In this regime, since l is much smaller than ℓ_{seg} , most bins overlap with only one MRCA segment and genealogies within a given bin are identical. Since ℓ_{seg} is much smaller than L , σ_l^2/μ_l can be calculated assuming independent genealogies for each bin. The result can be obtained from eq. (11) in the limit of $C \rightarrow 0$:

$$\sigma_l^2/\mu_l \simeq 1 + l/\Delta. \quad (14)$$

This means that σ_l^2/μ_l exhibits a plateau as a function of ℓ_{seg} (its value is equal to $1 + l/\Delta$ and thus independent of ℓ_{seg} or R). Result (14) is shown as a dashed line in Figure 3a. The plateau is cut off by l for small values of ℓ_{seg} , and by L for large values of ℓ_{seg} .

3. There are on average l/Δ SNPs in a bin of size l . If ℓ_{seg} is much smaller than l , these SNPs are distributed over many MRCA segments. If the counts per MRCA segment were statistically independent, one would expect $\sigma_l^2 \propto \ell_{\text{seg}}$, and thus $\langle \sigma_l^2 \rangle$ to increase roughly proportional to ℓ_{seg} (eq. (11) shows that there are logarithmic corrections to this simple model). As ℓ_{seg} approaches l , this increase is cut off; $\langle \sigma_l^2 \rangle/\mu_l \rightarrow 1$ as $\ell_{\text{seg}} \rightarrow L$. If l is large ($l \lesssim L$), there is no plateau.

In summary, σ_l^2/μ_l reflects local SNP clustering. It is expected to be most significant in the regime $\Delta < \ell_{\text{seg}} \ll L$. In many organisms S is of the order of R . For $n = 2$ eq. (8) implies that ℓ_{seg} is roughly 1.5Δ . In such cases, recombination alone gives rise to SNP clustering.

This clustering is observed on length scales of the order of ℓ_{seg} . Eq. (11) shows that its effect on $\langle \sigma_l^2 \rangle/\mu_l$ is most clearly seen if $l > \ell_{\text{seg}}$ (compare Fig. 3b). This observation has two important consequences: (1) in empirical situations it is advisable to choose the bin size l at least as large as ℓ_{seg} ; (2) deviations from the model considered may be associated with length scales much longer than ℓ_{seg} . Such deviations will be most clearly seen if the bin size l is equal to or larger than this length. In short: the dependence of σ_l^2/μ_l on l indicates on which length scales clustering of SNPs occurs.

DATA ANALYSIS

In the following we discuss the implications of our analysis for the interpretation of SNP data from mouse and human. In both cases we ask whether the neutral model can be rejected.

Mouse data: In their survey of SNPs in mice, LINDBLAD-TOH *et al.* (2000) observed that SNPs were not distributed uniformly across the genome. A possible explanation for this is selective breeding, which has certainly taken place in the recent evolution of the mice strains investigated. On the other hand, the SNP clustering in mice might also be due to recombination alone.

Figure 4 shows the empirically determined value of σ_l^2/μ_l [for *M. m. domesticus* SNPs, see LINDBLAD-TOH *et al.* (2000)] in comparison with coalescent simulations for $\langle\sigma_l^2\rangle/\mu_l$. L was taken to be $1.6 \cdot 10^8$ bp, corresponding to the average chromosome length. A value for ℓ_{seg} can be estimated from the average recombination rate in mice, approximately 0.5 cM/Mb (NACHMAN and CHURCHILL, 1992). Here we assume an effective population size $N_e = 10000$. The average bin length l is the average length of the sequence tagged sites investigated, i.e. 118bp, smaller than Δ . SNP clustering on the scale of l is thus expected to be small. Moreover, since l is much smaller than ℓ_{seg} , $\langle\sigma_l^2\rangle/\mu_l$ is expected to exhibit a plateau as a function of ℓ_{seg} , at $\langle\sigma_l^2\rangle/\mu_l = 1.12$. While the plateau is found in the simulations (Figure 4), the empirically determined value of σ_l^2/μ_l deviates significantly from neutral expectations (Figure 4; $\sigma_l^2/\mu_l = 1.47$). This increase of σ_l^2/μ_l above the value expected under neutrality is consistent with the earlier conclusion that selection plays an important role in shaping the genome-wide distribution of polymorphisms in mice (LINDBLAD-TOH *et al.*, 2000). In order to demonstrate this more conclusively, long-range SNP data would be of great interest for two reasons: (1) the larger l , the larger deviations from Poisson statistics are expected (ideally, l would be of the order of ℓ_{seg}). Figure 4 shows the increase in neutral SNP clustering if l is increased to 5kb. (2) Selection may act on length scales greater than ℓ_{seg} and may thus contribute only weakly at very small values of l such as those corresponding to an average STS.

Human chromosome 6: The distribution of chromosome-wide human SNP data was empirically determined for $l = 460$ bp and $l = 200$ kb by THE INTERNATIONAL SNP MAP WORKING GROUP (2001). Figure 5a shows our coalescent simulations compared to the empirical data for these length scales. Consider first the case of $l = 460$ bp. In the simulations, $\langle\sigma_l^2\rangle/\mu_l$ exhibits a plateau for intermediate values of ℓ_{seg} at $\langle\sigma_l^2\rangle/\mu_l \simeq 1.34$ [according to eq. (14)]. This implies that the choice of ℓ_{seg} attributed to the empirical value is uncritical. Empirically, $\sigma_l^2/\mu_l = 1.44$. From Figure 5a we conclude: given the degree SNP clustering observed in the human genome on scales of the order of $l = 460$ bp, the neutral model cannot be rejected with confidence.

The situation for $l = 200$ kb is very different. In this case, the simulation results do not exhibit a plateau. The numerical results indicate that $\langle\sigma_l^2\rangle/\mu_l$ increases roughly with ℓ_{seg} (for $\ell_{\text{seg}} \ll l$), as suggested above. Furthermore, the empirical value for σ_l^2/μ_l (labeled (1) in Figure 5a) lies significantly above the values for the neutral infinite-sites model with recombination [the corresponding value of ℓ_{seg} was estimated assuming an effective population size of $N_e = 10000$ and a recombination rate of 1 cM/Mb (PRITCHARD and PRZEWORSKI, 2001)]. This deviation is possibly caused by selection: the HLA system, which contains more than 100 genes and spans more than 4 Mb on the short arm of chromosome 6 (KLEIN *et al.*, 1993), has an exceptionally high SNP density. This is maintained by balancing selection (THE INTERNATIONAL SNP MAP WORKING GROUP, 2001; O’HUGIN *et al.*, 2000). The inset of Figure 5a shows the empirically determined distribution of the number of SNPs per bin $P(n(l) = k)$. It exhibits a strong tail for large values of k , which may be due to selection. By ignoring this tail the estimate (labeled (2) in Figure 5a) for σ_l^2/μ_l is reduced considerably. Given the uncertainty as to which value of ℓ_{seg} should be assigned to the data points, one may argue that this second estimate is

consistent with the neutral infinite-sites model.

Human X chromosome: Finally, Figure 5b shows the empirical estimate of σ_l^2/μ_l given $l = 200\text{kb}$ for the X chromosome. This empirical estimate was reduced by discarding the tail in the distribution $P(n(l) = k)$ for large k as was done in the analysis of the chromosome 6 data. However, both estimates of SNP clustering on the human X chromosome deviated significantly from neutrality. This observation is consistent with the fact that due to its hemizygoty in males chromosome X should be affected more by selection than autosomes such as chromosome 6.

DISCUSSION

In this paper we investigate whether the observations of SNP clustering in mice and humans are compatible with neutral expectations. We chose the variance in the number of SNPs found in equal-length contiguous divided by the mean number of SNPs found in each bin as a measure of SNP clustering: σ_l^2/μ_l . Since under a Poisson distribution the variance is equal to the mean, $\sigma_l^2/\mu_l = 1$ in the absence of recombination. If SNPs are clustered, $\sigma_l^2/\mu_l > 1$.

Whether or not SNP clustering is significant depends on the relative sizes of the mean spacing between neighboring SNPs, Δ , the mean length of segments with constant time to the most recent common ancestor, ℓ_{seg} , and the total length of the chromosome, L . Specifically, clustering is observed if $\Delta < \ell_{\text{seg}} \ll L$. In contrast, if recombination is either very frequent compared to mutation ($\ell_{\text{seg}} \ll \Delta$) or very rare ($\ell_{\text{seg}} \ll L$), no clustering is observed³.

We have shown that it is essential to consider the effect of the scale on which SNPs are sampled, l . In our simulations l describes the length of contiguous non-overlapping bins. This length is short compared to the length of the chromosome, and the corresponding large number of such bins leads to narrow confidence intervals around σ_l^2 for the biologically relevant parameters. As a result, meaningful comparisons between model and observation can be made. In the case of the mouse, the neutral model is rejected with marginal significance. This conclusion depends on the assumption of a “true” recombination rate for mice. This is difficult to know, but Figure (4) shows that our hypothesis test is quite robust with respect to errors in the estimation of R (and hence ℓ_{seg}).

In the case of human chromosome 6, the influence of l on the outcome of the neutrality test was striking. Significant SNP clustering was observed for large but not for small l (Figure 5a). For large bins ($l = 200\text{ kb}$) the distribution of the number of SNPs per bin had a strong positive skew (Figure 5a, inset). By cutting off the tail of bins containing many SNPs, clustering was reduced to its neutral level.

No such effect of cutting off the tail of SNP-dense bins was observed for the X-chromosome. It therefore constitutes the most significantly non-neutral SNP collection among the three data sets investigated in this study.

Factors that might lead to such a rejection of the neutral model include population expansion,

³Rather than the recombination rate R we use the corresponding length scale ℓ_{seg} as our point of reference for discussing SNP clustering; ℓ_{seg} can directly be compared to the other length scales of the problem, viz. the length of the bins in which SNPs are sampled in experiments, l , as well as Δ , and L . Moreover, equation (8) shows that ℓ_{seg} is a simple function of L , R , and the sample size n , thereby establishing the link between simulations conditioned on R and our observations.

population subdivision, and variation in (physical) mutation rate. In the case of the data sets we have investigated, some illuminating biology pertaining to these factors is known. LINDBLAD-TOH *et al.* (2000) tested whether unequal physical mutation rates could account for their observation of SNP clustering in mice. Their approach was to resequence 16 STSs with no SNPs and 16 STSs with five or more SNPs from closely related species of mice. They observed that the classification of high-scoring and low-scoring STSs was not reproduced in these other taxa and concluded from this that fluctuations in inherent mutation rates could not account for the observation of significant SNP clustering. The claim that selective breeding has been important in shaping the SNP distribution in mice is plausible, but other factors such as population expansion and subdivision can presumably not be ruled out.

The situation is slightly different in the case of human chromosomes 6 and X, where deviation from the neutral model was much more pronounced for the sex chromosome than for the autosome. Since all chromosomes have undergone the same history of population expansion and migration, selection seems to be the only explanation for this difference. The hemizyosity in males of the X-chromosome, which makes most deleterious mutations dominant in males, fits well with this conclusion.

ACKNOWLEDGEMENTS We would like to thank Richard Hudson for discussion and much appreciated comments on an earlier version of this manuscript. This work was supported by a grant from the Swedish Science Foundation.

References

- BERGER, J., SUZUKI, T., SENTI, K.-A., STUBBS, J., SCHAFFNER, G., and DICKSON, B. J., 2001 Genetic mapping with snp markers in *Drosophila*. *Nature Genetics* **29**: 475–481.
- CHO, R. J., MINDRINOS, M., RICHARDS, D. R., SAPOLSKY, R. J., ANDERSON, M., DRENKARD, E., DEWDNEY, J., REUBER, T. L., STAMMERS, M., FEDERSPIEL, N., THEOLOGIS, A., YANG, W.-H., HUBBELL, E., AU, M., CHUNG, E. Y., LASHKARI, D., LEMIEUX, B., DEAN, C., LIPSHUTZ, R. J., ASUBEL, F. M., DAVIS, R. W., and OEFNER, P. J., 1999 Genome-wide mapping with biallelic markers in *Arabidopsis thaliana*. *Nature Genetics* **23**: 203–207.
- FAY, J. C., WYCKOFF, G. J., and WU, C.-I., 2001 Positive and negative selection in the human genome. *Genetics* **158**: 1227–1234.
- GRIFFITHS, R. C. and MARJORAM, P., 1997 An ancestral recombination graph. volume 87 of *The IAM Volumes in Mathematics and its Applications*, pp. 257–270. Springer-Verlag, New York.
- HAUBOLD, B., KROYMANN, J., RATZKA, A., MITCHELL-OLDS, T., and WIEHE, T., 2002 Recombination and gene conversion in *Arabidopsis thaliana*. *Genetics* In press.
- HOSKINS, R. A., PHAN, A. C., NAEEMUDDIN, M., MAPA, F. A., RUDDY, D. A., RYAN, J. J., YOUNG, L. M., WELLS, T., KOPCZYNSKI, C., and ELLIS, M. C., 2001 Single nucleotide polymorphism markers for genetic mapping in *Drosophila melanogaster*. *Genome Research* **11**: 1100–1113.

- HUDSON, R. R., 1990 Gene genealogies and the coalescent process. *Oxford Surveys in Evolutionary Biology* **7**: 1–44.
- INTERNATIONAL HUMAN GENOME SEQUENCING CONSORTIUM, 2001 Initial sequencing and analysis of the human genome. *Nature* **409**: 860–921.
- KAPLAN, N. and HUDSON, R. R., 1985 The use of sample genealogies for studying a selectively neutral *m*-loci model with recombination. *Theoretical Population Biology* **28**: 382–396.
- KLEIN, J., TAKAHATA, N., and AYALA, F. J., 1993 Mhc polymorphism and human origins. *Scientific American* **269**: 78–83.
- LINDBLAD-TOH, K., WINCHESTER, E., DALY, M. J., WANG, D. G., HIRSCHHORN, J. N., LAVIOLETTE, J.-P., ARDLIE, K., REICH, D. E., ROBINSON, E., SKLAR, P., SHAH, N., THOMAS, D., FAN, J.-B., GINGERAS, T., WARRINGTON, J., PATIL, N., HUDSON, T. J., and LANDER, E. S., 2000 Large-scale discovery and genotyping of single-nucleotide polymorphisms in the mouse. *Nature Genetics* **24**: 381–386.
- MCINNES, L. A., SERVICE, S. K., REUS, V. I., BARNES, G., CHARLAT, O., JAWAHAR, S., LEWITZKY, S., YANG, Q., DUONG, Q., SPESNY, M., ARAY, C., ARAY, X., GALLEGOS, A., MEZA, L., MOLINA, J., RAMIREZ, R., MENDEZ, R., SILVA, S., FOURNIER, R., BATKI, S. L., MATHEWS, C. A., NEYLAN, T., GLATT, C. E., ESCAMILLA, M. A., LOU, D., GAJIWALA, P., SONG, T., CROOK, S., NGUYEN, J. B., ROCHE, E., MEYER, J. M., LEON, P., SANDKUIJL, L. A., FREIMER, N. B., and CHEN, H., 2001 Fine-scale mapping of a locus for severe bipolar mood disorder on chromosome 18p11.3 in the costarican population. *Proceedings of the National Academy of Sciences, USA* **98**: 11485–11490.
- NACHMAN, M. W. and CHURCHILL, G. A., 1992 Heterogeneity in rates of recombination across the mouse genome. *Genetics* **142**: 537–548.
- NORDBORG, M., 2001 Coalescent theory. In *Handbook of Statistical Genetics*, edited by D. J. BALDING, M. BISHOP, and C. CANNINGS, chapter 7, pp. 178–212. Wiley.
- NORDBORG, M. and TAVARÉ, S., 2002 Linkage disequilibrium: what history has to tell us. *Trends in Genetics* **18**: 83–90.
- O’HUGIN, C., SATTI, Y., HAUSMANN, A., DAWKINS, R., and KLEIN, J., 2000 The implications of intergenic polymorphism for major histocompatibility complex evolution. *Genetics* **156**: 867–877.
- PLUZHNIKOV, A. and DONNELLY, P., 1996 Optimal sequencing strategies for surveying molecular genetic diversity. *Genetics* **144**: 1247–1262.
- PRITCHARD, J. K. and PRZEWORSKI, M., 2001 Linkage disequilibrium in humans: models and data. *American Journal of Human Genetics* **69**: 1–14.
- THE INTERNATIONAL SNP MAP WORKING GROUP, 2001 A map of human genome sequence variation containing 1.42 million single nucleotide polymorphisms. *Nature* **409**: 928–933.

- WILLEY, J. S., DAO-UNG, L. P., SLUYTER, R., SHEMON, A. N., LI, C., TAPER, J., GALLO, J., and MANOHARAN, A., 2002 A loss-of-function polymorphic mutation in the cytolytic *P2X7* receptor gene and chronic lymphocytic leukaemia: a molecular study. *The Lancet* **359**: 1114–1119.
- WIUF, C. and HEIN, J., 1999 The ancestry of a sample of sequences subject to recombination. *Genetics* **151**: 1217–1228.
- ZHOU, W., GOODMAN, S. N., GALIZIA, G., LIETO, E., FERRARACCIO, F., PIGNATELLI, C., PURDIE, C. A., PIRIS, J., MORRIS, R., HARRISON, D. J., PATY, P. B., CULLIFORD, A., ROMANS, K. E., MONTGOMERY, E. A., CHOTI, M. A., KINZLER, K. W., and VOGELSTEIN, B., 2002 Counting alleles to predict recurrence of early-stage colorectal cancers. *The Lancet* **359**: 219–225.

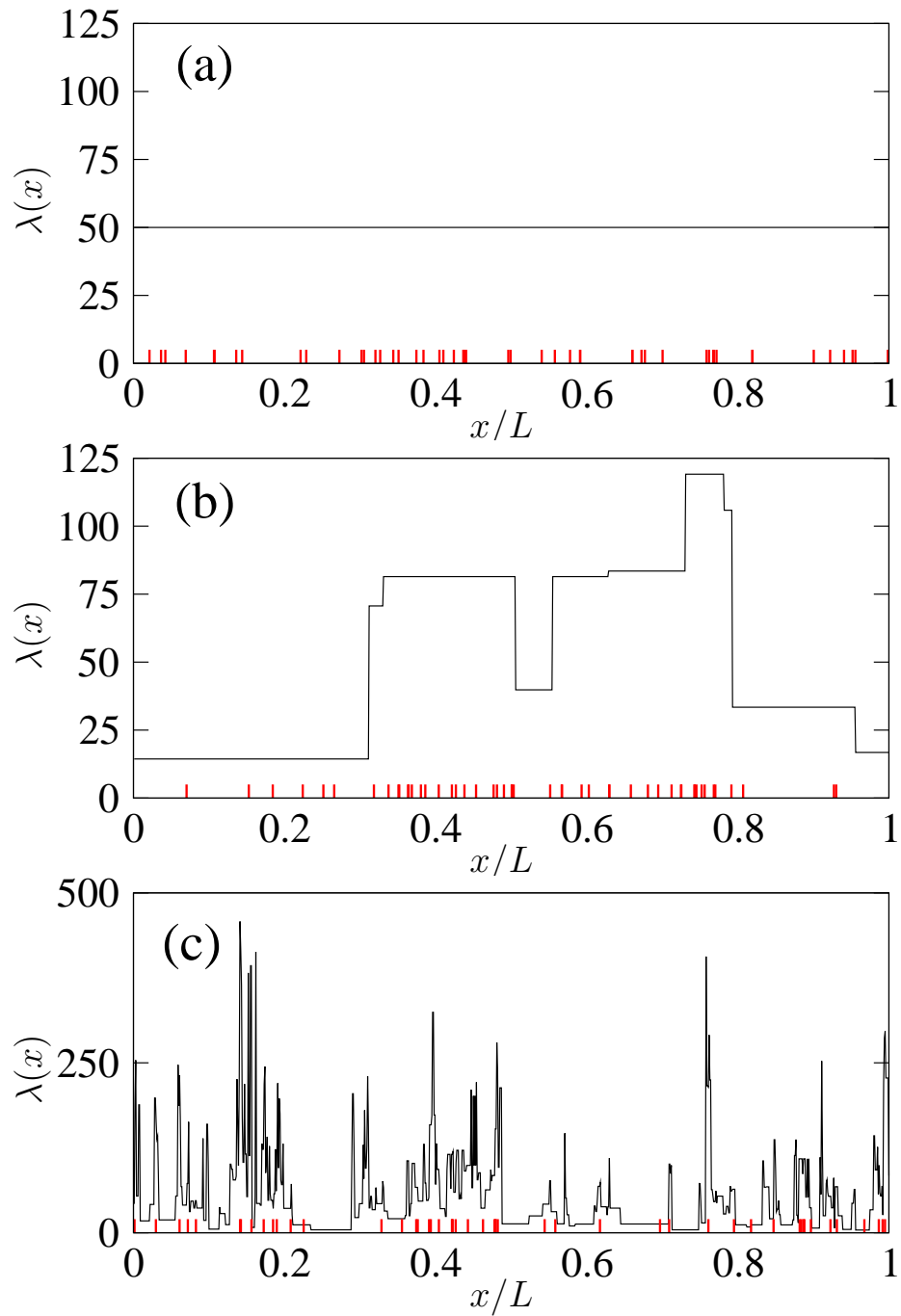


Figure 1: Recombination leads to spatial fluctuations in local coalescent times, $T_{\text{tot}}(x)$ (HUDSON, 1990), which in turn cause fluctuations of the local mutation rate $\lambda(x)$ (solid lines). Shown are three realizations of $\lambda(x)$ together with the locations of $S = 50$ SNPs (vertical bars) for $n = 2$ and (a) $R = 0$, (b) $R = 10$, and (c) $R = 1000$.

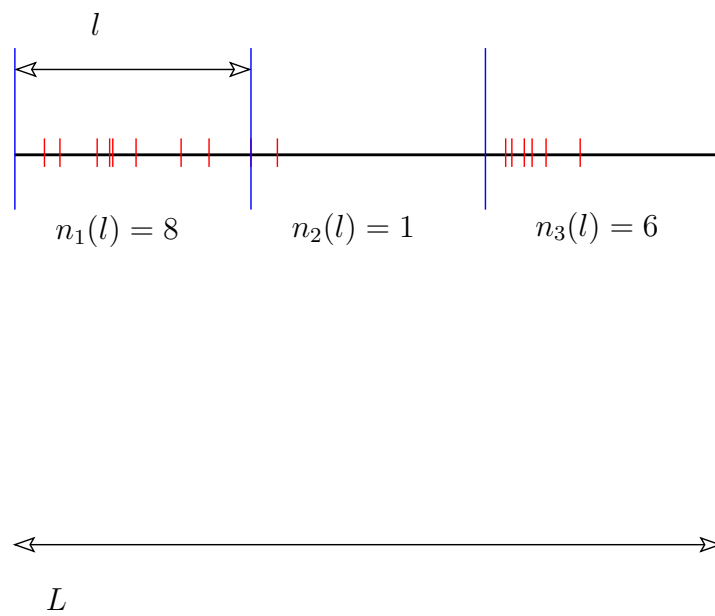


Figure 2: A chromosome of length L is divided into contiguous bins of length l . The number of SNPs in bin j is denoted by $n_j(l)$.

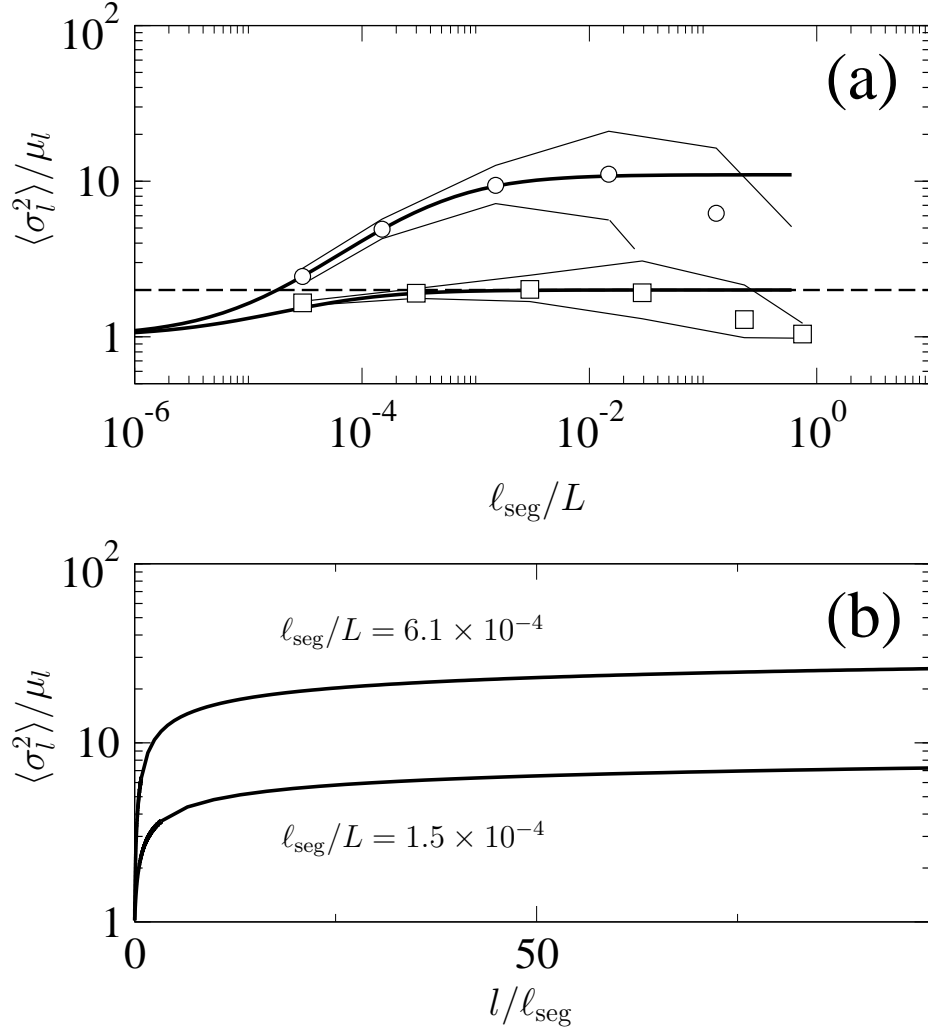


Figure 3: Coalescent results for $\langle \sigma^2 \rangle / \mu_l$ (open symbols) in comparison with eq. (11) (thick lines). Thin lines indicate 90% confidence intervals. (a) $\langle \sigma_l^2 \rangle / \mu_l$ for $n=2$ and $\Delta/L = 10^{-4}$, as a function of ℓ_{seg}/L for $l/L = 10^{-4}$ and $l/L = 10^{-3}$ (\circ). Also shown are the values of σ_l^2 / μ_l from eq. (14) for $l/L = 10^{-4}$ (---). (b) $\langle \sigma_l^2 \rangle / \mu_l$ for $n=2$ and $\Delta/L = 10^{-4}$.

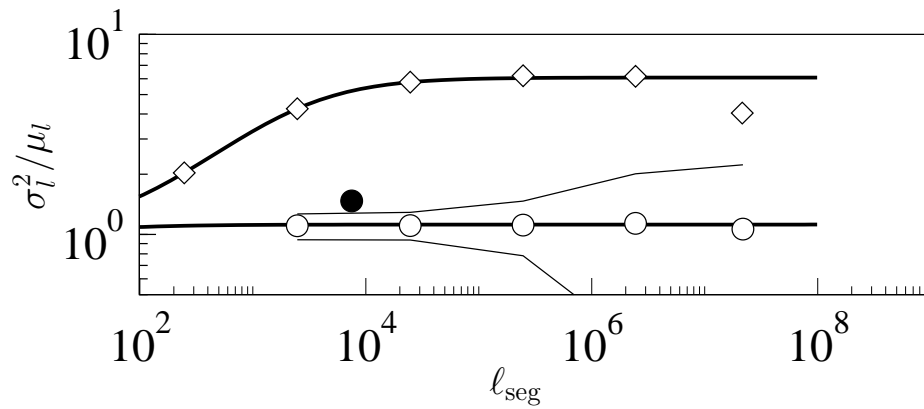


Figure 4: σ_l^2/μ_l for *M. m. domesticus* SNPs (LINDBLAD-TOH *et al.*, 2000) (\bullet). Simulation results for $\langle \sigma_l^2 \rangle / \mu_l$ are shown, corresponding to $l = 118\text{bp}$ (\circ) – the average read length in (LINDBLAD-TOH *et al.*, 2000) – and corresponding to $l = 5\text{kb}$ (Diamond). In addition, the results according to eq. (11) (thick lines), and, for $l = 118\text{bp}$., 90% confidence intervals (thin lines) are shown.

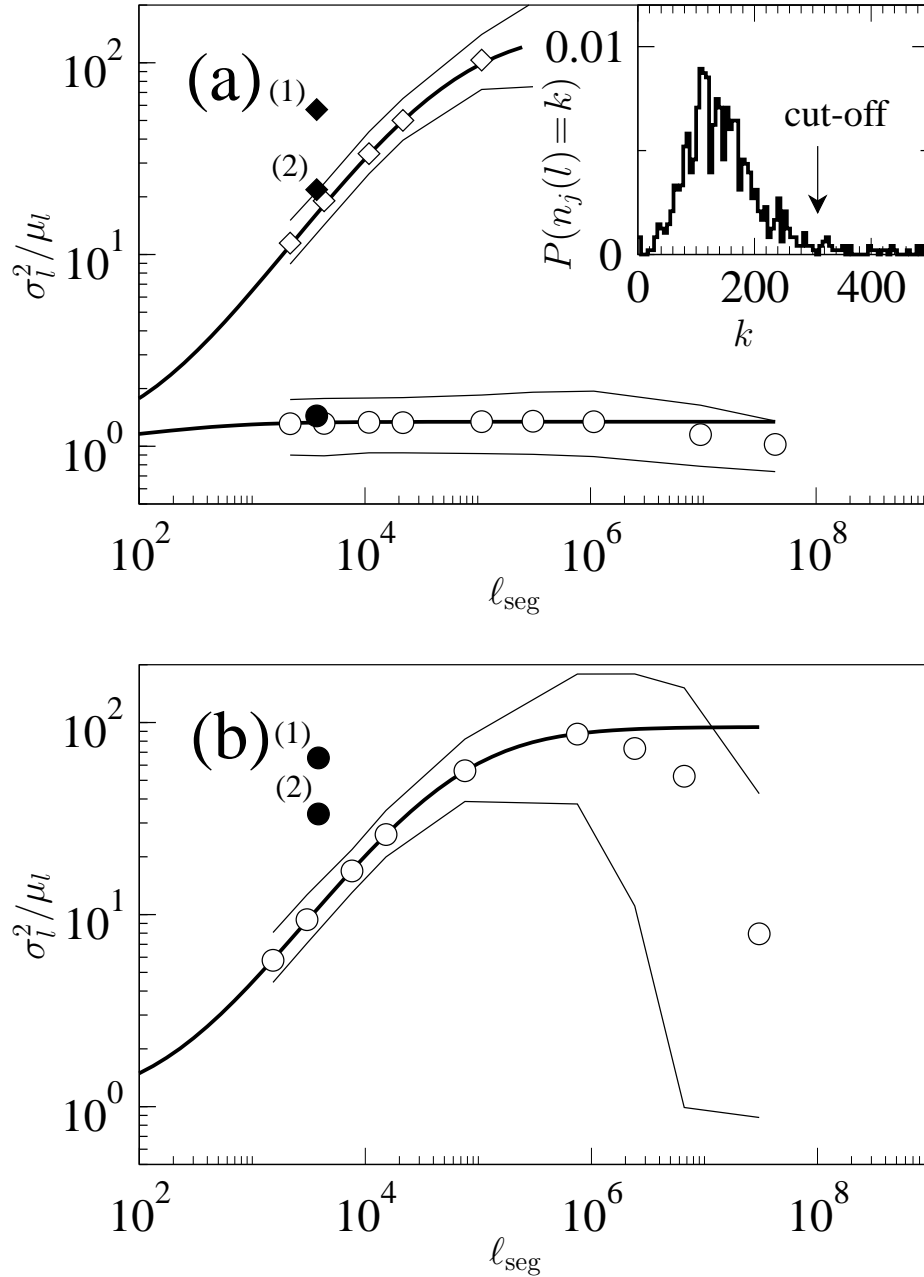


Figure 5: (a) Variance of SNPs for chromosome 6 in the human genome. Empirical data for bin sizes $l = 460\text{bp}$ (\bullet) and $l = 200\text{kb}$ (\blacklozenge) are determined from the data provided by THE INTERNATIONAL SNP MAP WORKING GROUP (2001). The data points labeled by (1) and (2) differ by a choice of cut-off (see text). Also shown are the mean results of coalescent simulations corresponding to $l = 460\text{bp}$ (\circ) and $l = 200\text{kb}$ (Diamond) and their 90% confidence intervals (thin lines), compared to theoretical expectations from (11) (thick lines). The inset shows the empirical distribution of $n_j(l)$ corresponding to $l = 200\text{kb}$. (b) Variance of SNPs for the human X chromosome. Empirical data for $l = 200\text{kb}$ (\bullet) were determined from the data provided by THE INTERNATIONAL SNP MAP WORKING GROUP (2001). Also shown are mean results of coalescent simulations corresponding to $l = 200\text{kb}$ (\circ), and their 90% confidence intervals (thin lines) compared to theoretical expectations from equation (11) (thick line).